Parallel Operation of Transformers with On Load Tap Changer and Photovoltaic Systems with Reactive Power Control

M. Kraiczy, T. Stetz, M. Braun (Senior Member)

***Abstract*—In recent years, the number of active grid components for voltage regulation in distribution grids has increased significantly. Besides voltage regulators (VRs), such as transformers with On Load Tap Changers (OLTCs), distributed generators can provide a certain voltage support by means of reactive power control (RPC). The different control entities, OLTC and RPC by photovoltaic (PV) systems, usually operate based on local measurements and control characteristics. Hence, unintended interactions between the control entities cannot be excluded in general. This study analyses the parallel operation of OLTC transformers with a voltage based control and PV systems with different RPC strategies (e.g. watt/power factor control PF(P), volt/var control (Q(V)) in a distribution system environment. The focus is on unintended interactions, such as an increase of OLTC switching operations by PV RPC. The contribution and novelty of this paper is to raise awareness for the likelihood of these unintended interactions and to provide a first methodology to assess the parallel operation of OLTC control and PV RPC in detail. The results show that the impact of PV RPC on the number of OLTC switching operations and the effectiveness in parallel operation can differ considerably between the applied PV RPC strategies.**

***Index Terms*—voltage regulation, reactive power control, on load tap changer, voltage support, volt/ var control**

I. Introduction

The electric power supply systems in various countries are undergoing a change towards a high share of renewable energy sources (RES). The worldwide RES capacity increased from 950 GW in the year 2004 to 1,990 GW in 2015 [1]. A high share of the RES, such as photovoltaic (PV) systems, is connected to the distribution grid and hence can be characterized as distributed generators (DGs). One major challenge for distribution system operators (DSOs) is the voltage regulation in distribution grids with a high DG penetration. Advanced DG functions (e.g. [2], [3]) like reactive power control (RPC) for voltage support can help to reduce the impact of DG feed in on the local voltage magnitude. Studies (e.g. [4]–[7]) show that the application of DG RPC can increase a grid's hosting capacity for DG feed in, for instance, and hence avoid or at least delay grid reinforcement measures. In the studies [6] and [7], the impact of DG RPC on the grid hosting capacity is also analyzed for different OLTC control strategies. These studies highlight that advanced OLTC configurations and DG RPC have high potential to improve the voltage regulation in distribution grids with a high DG penetration. Nowadays, DSOs in several countries are taking advantage of the grid support functionalities of state of the art DG by requiring RPC in their interconnection guidelines (e.g. [8] to [11]).

However, the IEEE working group on distributed generation integration expressed its concerns that DG RPC could conflict with other voltage regulation schemes applied by the DSO [13]. The study [14] showed, that a volt/var control (Q(V) control) can operate stably under all grid condition, if the Q(V) control settings are appropriately. However, the focus in [14] was not set on the parallel operation with other voltage regulators (VRs). In the literature, especially the parallel operation of DGs and VRs operating with a line drop compensation (LDC) algorithm were analyzed in detail (e.g., [15] to [17]). In Germany and other European countries, a voltage-based control method is usually applied for VRs, like OLTC transformers. Also the German Grid Technology/Grid Operation Forum (FNN) identified a research gap in parallel operation of DG RPC with OLTC transformers [12]. So far, a few studies have addressed the parallel operation of OLTC control and DG RPC in detail. The analysis in [18] showed that PV RPC can lead to a significant increase of reactive power fluctuations over the OLTC transformer and therefore to increased voltage fluctuations at the secondary transformer busbar. These voltage fluctuations can cause a relevant increase of OLTC transformer switching operations. The study in [19] evaluates different time delay algorithms for OLTC control and their effectiveness in grids with high DG penetration regarding the objective of minimizing the number of OLTC switching operations and keeping the voltage within the permissible bandwidth.

The contribution and novelty of the paper at hand is to raise awareness for the likelihood of unintended interferences between autonomously controlled entities in the context of smart grids (such as volt/var control and OLTC operation, for example). The focus is set on the following interferences:

- unintended OLTC switching operations caused by PV RPC,
- increase of the number of OLTC switching operations caused by PV RPC.

M. Kraiczy is with the Fraunhofer Institute for Wind Energy and Energy System Technology IWES (e mail: markus.kraiczy@iwes.fraunhofer.de), 34119 Kassel, Germany. T. Stetz is Professor at the Technische Hochschule Mittelhessen, 35390 Gießen, Germany. M. Braun is Professor at the University of Kassel, 34125 Kassel, Germany, and also with Fraunhofer IWES, 34119 Kassel, Germany.

This article has been accepted for publication in a future issue of this journal, but has not been fully edited. Content may change prior to final publication. Citation information: DOI 10.1109/TSG.2017.2712633, IEEE Transactions on Smart Grid

Therefore, the study provides a first methodology to assess the parallel operation of OLTC control and PV RPC in detail, aiming at identifying:

a) different kind of unintended interactions,
b) their likelihood in medium or high PV penetration scenarios with PV RPC,
c) suitable combinations of autonomous control characteristics and
d) sensitive parameters that can be tuned by respective DSOs in order to minimize the risk of unintended interactions as identified in a).

The paper is structured as follows: Section II depicts the simulation model with the PV, load, and OLTC configuration. In Section III, the technical background concerning the parallel operation of OLTC control and PV RPC is explained in detail and a first assessment is proposed to analyze the impact of PV RPC on the VR control. The technical assessment in parallel operation of OLTC control and PV RPC is presented in Section IV. In Section V a sensitivity analysis of grid and controller configurations is performed. Section VI discusses the simulation assumptions and the relevance of the presented findings. Finally, the conclusion of the study is presented.

II. Simulation Model

The focus of the study is set on identifying potential threats to the long term voltage stability in distribution grids where OLTC transformers and PV RPC are operated in parallel. Therefore, root mean square (RMS) simulations with the Software PowerFactory and a simulation step size of one second are performed. To aid comprehensibility, the simulations are performed on an open access benchmark grid. The grid is reconfigured for the case study of a German MV grid with high PV penetration. In the following subsection, the configuration of the grid model, the load models, the PV models, and the OLTC model are explained.

A. Grid Model

The grid simulations are performed on the CIGRE medium voltage (MV) benchmark grid (nominal voltage V_N = 20 kV), which was introduced and explained in [20]. The benchmark grid was designed for DG integration studies and is representative of a real German MV grid. For the study, only subnetwork 1 is considered. Additionally, the 110/20 kV substation transformer is equipped with an OLTC (see Table A1 in the Appendix). In the reference scenario, PV systems with a nominal power (nominal inverter power S_N = nominal PV module power under standard test conditions P_{PV_STC}) of 800 kWp are connected to every MV terminal. PV systems in the underlying LV grids are not considered in the case study. Worst case analyses are performed to validate the compliance of the chosen PV penetration scenario with the maximum permissible voltage bandwidth in the MV grid. In the sensitivity analysis in Section V, the PV penetration scenario and the positioning of the PV systems is varied.

Fig. 1 shows a single line diagram of the investigated MV grid (top) and the results of the worst case analysis (bottom). According to EN 50160, the maximum permissible voltage magnitude at the German MV and LV levels is 110% of V_N. In the grid scenario, the OLTC controls the voltage at T1 to 104% of V_N (±1% deadband). The maximum permissible voltage in the MV level is set to 107% of V_N and a voltage rise of 3% of V_N is reserved for the LV level. The maximum permissible voltage rise in the MV and LV level is allocated according to the maximum permissible voltage variation by DG systems, according [8] and [9]. The results of the worst case scenario maximum PV (power factor (PF) = 1) and low load (black line) already show a maximum MV grid voltage of 1.073 p.u. at terminal T11. Therefore, PV RPC is already required in the investigated PV penetration scenario.

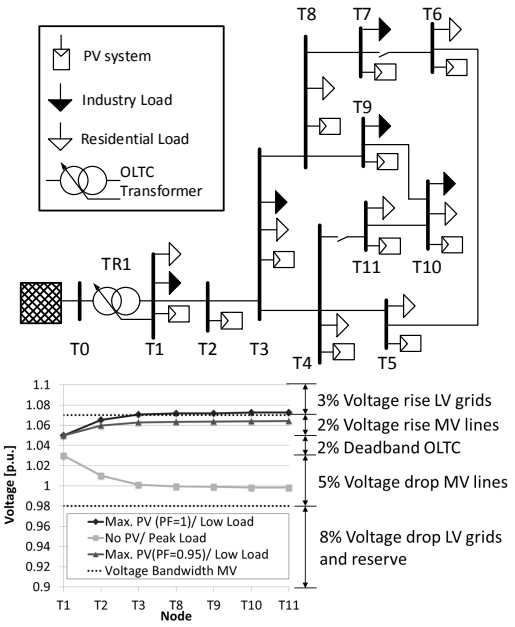

Fig. 1: MV grid based on the CIGRE MV benchmark grid [20] (top); results of the worst case analysis for the critical feeder T1–T11 (bottom); and the applied allocation of the voltage bandwidth for a German MV and LV grid (bottom, right). (PF = power factor)

B. Load Model

The electric loads are configured according to information with regard to the load type (household, industry) and its respective maximum active and reactive power consumption in [20]. For the RMS simulations, standard load profiles with a high comparability to the load profiles applied in [20] are used. Fig. 2 shows the applied load profiles for household and industry loads. The loads are simulated with a fixed power factor according to the given maximum active and reactive power values of the loads in [20]. The voltage dependence of the loads is simulated by a ZIP model for which the active and reactive power coefficients are derived from the mean values (European case: np = 0.55, nq = 0.91) of the analysis in [21].

C. PV Model

The solar variability in a grid area has a relevant impact on the active and reactive power fluctuations and gradients of a distributed PV fleet. Several studies show that the solar variability decreases significantly with increasing plant size ([22]–[24]); hence the solar variability is larger for a single residential scaled PV system compared with an aggregated PV fleet or utility size PV plant. However, the detailed modelling

This article has been accepted for publication in a future issue of this journal, but has not been fully edited. Content may change prior to final publication. Citation information: DOI 10.1109/TSG.2017.2712633, IEEE Transactions on Smart Grid

of an aggregated PV fleet with a high temporal resolution requires extensive measurement data from the analyzed grid area, which is usually not available. For the analyzed generic MV grid, no measurement data or geographical information for the PV fleet is available and a sensitivity analysis of the solar variability is performed.

For this purpose, a simplified approach based on the PV model in [22] is used. The study [22] shows that the application of a point sensor measurement with an optimized low pass filter (first order filter) can be used to estimate the smoothed power output of a large utility size PV plant or a distributed PV fleet. In [22], the optimal filter time constant (T) varies between 54 s (covered area: 0.12 km²) and 437 s (covered area: 36 km²). For the study at hand, the filter time constant (T) is varied between 0 s (no smoothing of solar variability) and 500 s (strong smoothing of solar variability). For the reference scenario, a filter time constant of 300 s is assumed and in Section V, a sensitivity analysis is performed for the solar variability. Fig. 2 (right) shows the maximum relative ramp rates (RR) of the applied PV generator profiles per capacity for different filter time constants (T). Detailed information and a flow chart for the preparation of the PV generation profiles are given in the Appendix Fig. A1. The simulations are performed for a clear sky day and a partially cloudy day with different filter time constants T (Fig. 3, left: T = 75 s, right: T = 300 s).

The applied inverter model was introduced in [25] and detailed information about the configuration of the PV inverter is given in the Appendix (Table A1). In this study, different RPC strategies are analyzed, namely:

- RPC Mode 1: No RPC (PF = 1);
- RPC Mode 2: Fixed power factor (PF = 0.95);
- RPC Mode 3: PF(P) control (watt/ power factor control);
- RPC Mode 4: Q(V) control (volt/ var control).

The characteristics of the PF(P) and Q(V) control are shown in Fig. 4. For the base scenario, version V1 (black line in Fig. 4) is applied. Only an underexcited operation of the PV inverters is considered.

D. OLTC controller

The OLTC of the HV/MV transformer controls the MV busbar voltage (V_{T1}) at a fixed set voltage (V_{OLTC_set}) of 104% of V_N. The OLTC controller is simulated with a voltage deadband (dV_{OLTC_BAND}) of ±1% around V_{OLTC_set} and a delay function. Fig. 5 (left) shows the applied delay functions. For the reference scenario, the version V1 of the delay function (black line in Fig. 5, left) is applied. The delay function avoids OLTC switching in cases of short term voltage variation. A further description of the OLTC controller setup is given in [25].

III. Preliminary Analysis: Parallel Operation of OLTC control and PV RPC

This section gives an overview of the technical background on parallel operation of OLTC control and PV RPC.

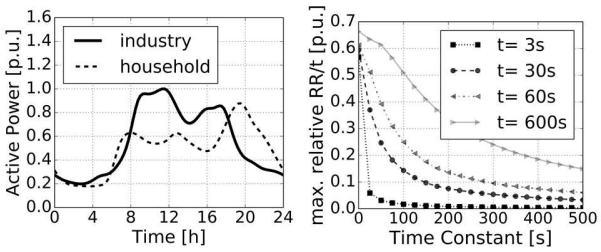

Fig. 2: left: applied standard load profiles for industry (black line) and household loads (dashed line); right: maximum relative ramp rates (RR) PV DC profiles (cloudy sky day) for different time intervals t and for different filter time constants T.

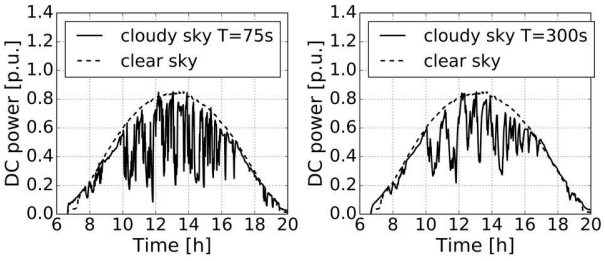

Fig. 3: Applied PV generation profiles for clear sky day (dashed line) and cloudy day (black line) for different filter time constants T (left: T = 75 s, right: T = 300 s)

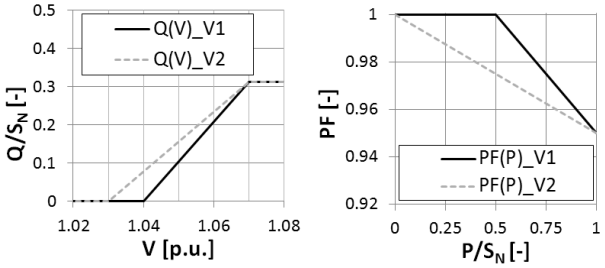

Fig. 4: Applied reactive power control strategies: Q(V) control (left) and PF(P) control (right) (only underexcited operation considered)

A. Short Circuit Power and R/X ratio in the MV Grid

In Fig. 5 (right), the short circuit power Sk'' and the R/X ratio at different nodes in the MV grid are shown. The nodes T6 and T11 are at the end of the feeders and are characterized by a relatively low Sk'' and a corresponding small X/R ratio. The voltage at busbar T1 is the control variable of the OLTC transformer. This busbar is characterized by a relatively large short circuit power and a large X/R ratio, due to the large serial inductance of the OLTC transformer impedance. Therefore, the voltage magnitudes at T6 and T11 (ends of the feeders) are especially sensitive to the active power flow, and the voltage magnitude at T1 (transformer substation) is especially sensitive to the reactive power flow.

B. Voltage Variations caused by PV Feed in in the MV Grid

In Fig. 6 the voltage variation caused by PV feed in is analyzed for nodes T11 and T1. Increasing the PV active power feed in leads to rising voltage magnitudes at T11 and PV RPC can reduce the voltage rise at T11 (Fig. 6, right). It should be noticed that the voltage at T1 is not significantly affected by the active power feed in of the PV systems. However, an increased reactive power provision by the PV systems (underexcited) can lead to a significant voltage drop at node T1 (Fig. 6, left). Therefore, PV RPC can increase the

This article has been accepted for publication in a future issue of this journal, but has not been fully edited. Content may change prior to final publication. Citation information: DOI 10.1109/TSG.2017.2712633, IEEE Transactions on Smart Grid

voltage variations |dV| at T1 and might lead to an increase of the number of OLTC switching operations.

C. Reactive Power Fluctuations caused by PV Systems

For PV systems, the active power feed in and hence also the reactive power provision can vary greatly over time. In a previous study [18], the impact of PV RPC on the reactive power ramp rates at the HV/MV transformer was analyzed for a real German distribution grid. The results in [18] showed that PV RPC can significantly increase the reactive power ramp rates and hence increase reactive power fluctuations over the HV/MV transformer, especially on days with a highly variable irradiation. The highest reactive power ramps were determined for the PF(P) control [18]. In Fig. 7 (left), the reactive power provision is shown as a function of the active power provision according to the applied characteristics for the fixed PF control (PF = 0.95) and PF(P) control. High reactive power ramps are determined for the PF(P) control (PF(P)_V1) with 0.58 var/W (at $P/S_N = 0.75$) compared with 0.33 var/W for the fixed PF control (PF = 0.95).

D. Voltage Dependency of Q(V) Control

In Fig. 7 (right), the reactive power provision by all MV PV systems (grayscale) is shown for different voltages at T1 for the Q(V) control. For this analysis, the slack voltage was set on the MV busbar T1 and the OLTC control was deactivated. The fixed power factor control and the PF(P) control are voltage independent. This is not the case for the Q(V) control. Due to the voltage dependency of the Q(V) control, the Q(V) control is also influenced by the voltage at T1. In the case of a high voltage at T1, the Q(V) control will likely provide more reactive power to reduce the voltage in the grid. Therefore, the Q(V) control can reduce the risk of exceeding the upper OLTC threshold (upper dashed line in Fig. 7, right). Otherwise, in the case of a low voltage at T1, the Q(V) control will likely provide less reactive power. Therefore, the risk of triggering an additional OLTC switching operation at the lower OLTC threshold (lower dashed line in Fig. 7, right) is reduced for the Q(V) control. The voltage dependency of the Q(V) characteristic also tends to smooth voltage variations at the OLTC transformer (T1).

E. First Assessment for the parallel operation of Voltage Regulators and PV Reactive Power Control

The analysis in Fig. 6 already allows a first assessment for the parallel operation of VR control and PV RPC, in general. First, it is assumed that the VR controller has a fixed voltage set point or a fixed voltage range (voltage mode) at a specific grid node. In case the VR controls the voltage at a weak grid node (low Sk'' and low X/R ratio, e.g. T11); PV RPC can reduce the voltage variations |dV| (Fig. 6, right) at this node and the application of PV RPC will likely reduce the number of VR switching operations. This can be the case for line voltage regulators or switched capacitors situated at a weak grid node (low Sk'' and low X/R). This can also be the case for VR control strategies, which control the voltage at a remote or distant grid node (e.g. line drop compensation mode). However, for the line drop compensation mode it is important that the VR calculates the voltage at the distant grid node correctly (direction detection of active and reactive power flow) in order to keep the voltage at the distant node within the specified limits.

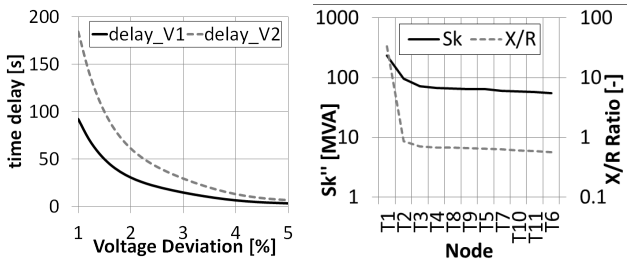

Fig. 5: Applied delay function (delay V1, delay V2) of the OLTC controller (left). Short circuit power Sk'' and X/R ratio at different grid nodes for the MV grid (right, logarithmic scale).

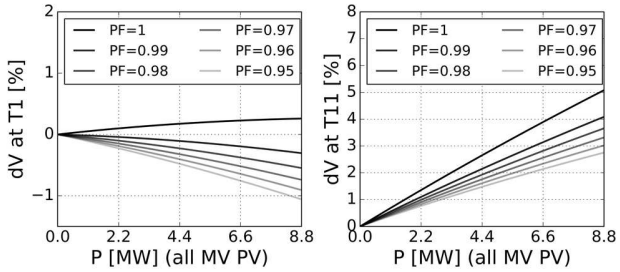

Fig. 6: Voltage variations dV at node T1 (left) and node T11 (right) caused by all PV systems. (Assumptions: slack voltage = 1.0 p.u. at T0, OLTC control deactivated, low load case, reference for dV: $P_{PV} = 0$ MW)

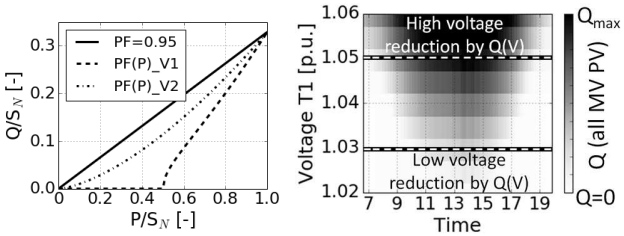

Fig. 7: Special issues of RPC strategies. Left: high Q gradients (dQ/dP) especially for the PF(P) control (PFP_V1); right: Q provision of MV PV (grayscale) with Q(V) control for different voltages at T1 at the clear sky day. The white dashed lines represent the OLTC thresholds at T1.

The paper at hand focus on a VR (OLTC transformer), which controls the voltage at a rather strong grid node (high Sk'', high X/R ratio, e.g. T1). Whereby the voltage at this node is especially sensitive to the reactive power flow and PV RPC will increase voltage variations |dV| at this node (Fig. 6, left). The findings of the paper at hand regarding the parallel operation of VR control and PV RPC are relevant, in case of:

- The VR controller has a fixed voltage set point or fixed voltage range at a specific grid node,
- PV RPC leads to an increase of voltage variations at the controlled grid node.

This can be the case for different kind of VR (e.g. OLTC transformer, line voltage regulators, switched capacitors). However, the dynamic behavior of the different VR may differ from the here analyzed OLTC application.

IV. Technical Assessment: Parallel Operation of OLTC control and PV RPC

In this section, the applied methodology is introduced and the technical assessment for the parallel operation of OLTC control and PV RPC is presented.

This article has been accepted for publication in a future issue of this journal, but has not been fully edited. Content may change prior to final publication. Citation information: DOI 10.1109/TSG.2017.2712633, IEEE Transactions on Smart Grid

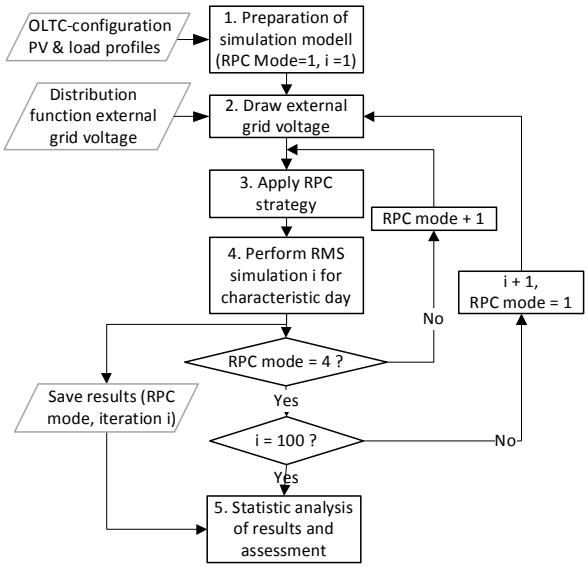

Fig. 8: Methodology for the assessment of the parallel operation of OLTC control and PV RPC

A. *Methodology*

The applied methodology is based on a Monte Carlo simulation of the external grid voltage. An overview of the applied methodology is given in Fig. 8. Besides the active and reactive power flow over the HV/MV transformer, the voltage at the upstream HV busbar (V_{T0}) also has a relevant impact on the OLTC operation. It is common practice to set the slack voltage at the external grid to a fixed value (e.g. 1.0 p.u.). However, this choice of external slack voltage has a relevant influence on the point in time and the number of OLTC switching operations. This impact is explained more in detail in the Appendix Fig. A3. The Monte Carlo simulation is therefore required to increase the reliability of the analysis and to avoid a very case specific outcome for just one specific external grid voltage setting. The single steps of the applied methodology are explained below:

1. The OLTC control is configured; the load and PV profiles are implemented (compare Section II). PV RPC is set to Mode 1 (PF=1) and the Monte Carlo iteration counter i is set to 1.
2. The slack voltage of the external grid is drawn from a specified distribution function, namely, a normal distribution with parameters μ=1.0 p.u., σ=0.05 p.u. (see Table A1). Overall, approximately 99% of the drawn values are within the permissible voltage range (long term voltage variations) for the German HV grid [29].
3. The respective PV RPC mode is applied for all MV PV.
4. The RMS simulation is performed for the characteristic day with the applied PV RPC mode and the drawn slack voltage. The simulation is repeated for all four PV RPC modes (RPC mode +1) with identical grid configurations. In case all RPC modes were simulated (RPC mode =4?) a new monte carlo iteration (i = i+1) is started, the RPC mode is set to 1 and a new external grid voltage is drawn. Overall, 100 Monte Carlo iterations are performed for each RPC mode.

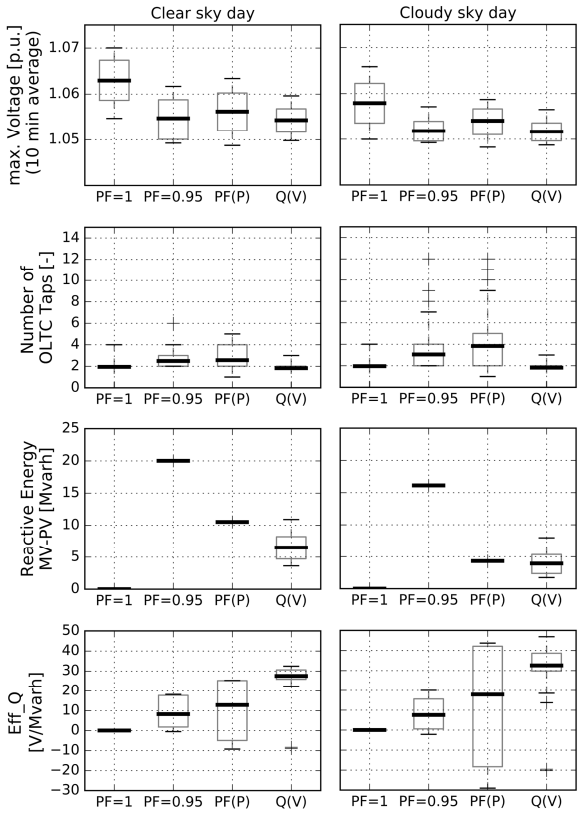

Fig. 9: Box plots of the Monte Carlo simulation for the clear sky day (left) and the cloudy day (right). The black bars define the mean values; the boxes define the 25 and 75% percentiles of the result population.

5. Finally, a statistic analysis and assessment of the parallel operation of OLTC control and PV RPC is performed.

The technical assessment is performed according to the criteria of maximum voltage magnitude (of all MV grid nodes), additional OLTC switching operations, and the PV reactive energy provision (aggregated for all MV PV). Furthermore, an effectiveness ratio Eff_Q is introduced (Eq. 1-2). The effectiveness ratio compares the "benefit" of PV RPC, being the reduction of the maximum grid voltage, with the "effort" of PV RPC, being an additional reactive power provision by the PV systems. Additional reactive power provision by PV leads to an increase of PV inverter losses and might lead to an overloading of grid assets, additional network losses, and further expenses for reactive power balancing (e.g. [30]). In Figure A2 in the Appendix the grid losses are shown for the different PV RPC strategies. The additional grid losses by PV RPC correlate with the reactive power provision of the PV systems for the analyzed MV grid. In order to avoid unnecessary grid losses a high effectiveness ratio Eff_Q should be achieved. In summary, these equations are:

$$eff\_Q_{mode,i} = \frac{[V_{\max}]_{PF1,i} - [V_{\max}]_{mode,i}}{[Q_{PV}]_{mode,i}} \quad (1)$$

$$Eff\_Q_{mode} = mean\{[eff\_Q_{mode,i}]_{i=1,\ldots,100}\} \quad (2)$$

where:

- V_{max}: maximum MV grid voltage for simulation i;

This article has been accepted for publication in a future issue of this journal, but has not been fully edited. Content may change prior to final publication. Citation information: DOI 10.1109/TSG.2017.2712633, IEEE Transactions on Smart Grid

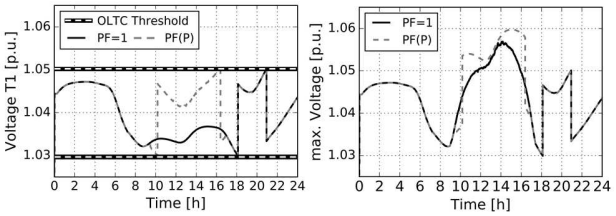

Fig. 10: Voltage at T1 (left) and the maximum MV grid voltage (right) in the case of a contrary operation of OLTC control and PV RPC with PF(P) control (example for the clear sky day).

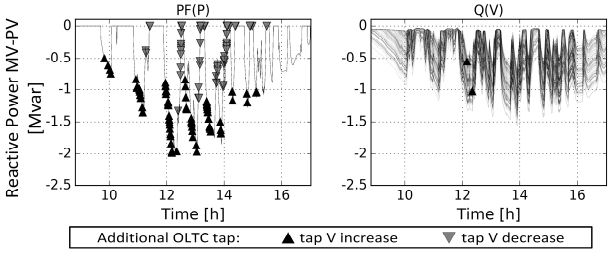

Fig. 11: Q provision of PV systems for the PF(P) control (left) and Q(V) control (right) and the points in time of additional triggered OLTC switching operations for the cloudy sky day (100 Monte Carlo iterations).

- Q_{PV}: reactive energy supplied by all MV PV systems for simulation i;
- i: index referred to Monte Carlo simulation (i=1,…,100)
- mode: index referred to the applied RPC strategy;
- PF1: index referred to the scenario with PF = 1.

B. *Results for Clear Sky Day and Cloudy Day*

The results of the Monte Carlo analysis are shown by the box plots in Fig. 9. The black bar defines the mean value of the result population. The maximum voltage (Fig. 9, top) considers the voltage of all MV nodes (T1 to T11). The results show a relevant voltage reduction potential for all types of PV RPC. The highest mean voltage reduction potential is determined for the fixed PF control (PF = 0.95) and the Q(V) control (Fig. 9, top). However, the fixed PF control (PF = 0.95) also leads to the highest reactive energy provision from all PV systems and consequently shows the lowest mean effectiveness ratio Eff_Q of 8 V/Mvarh, compared to 17 V/Mvarh for the PF(P) control and 33 V/Mvarh for the Q(V) control on the cloudy day.

Especially on the cloudy day, the fixed PF control (PF = 0.95) and the PF(P) control lead to an increase of OLTC switching operations. The mean number of OLTC switching operations increases from 1.9 (PF = 1) to 3.1 (PF = 0.95, +63 %) and to 3.8 (PF(P), +100 %) for the cloudy day. Otherwise the Q(V) control leads to a slight decrease to 1.8 OLTC switching operations (5%) in average. This effect is even more significant for the maximum number of OLTC switching operations, which increases from 4 (PF = 1) to 12 operations (PF(P) and PF = 0.95) for the cloudy day.

Furthermore, the effectiveness ratio $eff_{\_Q}$ is negative for some of the Monte Carlo iterations with the PV RPC strategies (Fig. 9, bottom). For these simulations, PV RPC leads to an increase of the maximum grid voltage compared with the scenario PF = 1 (compare Eq. 1). This effect is especially significant for the PF(P) control, which is discussed more in detail in the next section.

C. *Additionally Triggered OLTC Tap Changes*

Fig. 10 shows an example of an unintended OLTC switching operation, caused by PV RPC with PF(P) control. The additional reactive power provision of the PV systems (underexcited) leads to an additional voltage drop at the OLTC transformer V_{T1}, and at 10 a.m. an unintended OLTC switching operation is triggered to compensate the voltage drop at T1 (Fig. 10, left). As a consequence, the maximum MV grid voltage is higher with PF(P) control (Fig. 10, right) compared to the base case scenario (PF = 1). Hence in this simulation example, the PF(P) control achieves a negative effectiveness ratio eff_Q.

In Fig. 11, the reactive power provided by all MV PV systems and the points in time with additional triggered OLTC switching operations are shown for the PF(P) control (left) and the Q(V) control (right) for the partly cloudy day and for 100 Monte Carlo iterations. Additional OLTC switching operations that increase the grid voltage (Fig. 11, dark gray triangles) are especially determined for points in time with a medium or high reactive power provision of the PV systems. The reactive power provision of the PV systems aims to lower the grid voltage. Therefore, the unintended OLTC switching operations caused by PV RPC usually decrease the effectiveness ratio Eff_Q. For most of the simulations, the Q(V) control shows no effect on the number of OLTC switching operations (Figs. 9 and 11) and achieves the highest effectiveness ratio in parallel with the OLTC control (Fig. 9). The risk of unintended OLTC switching operations is significantly reduced by the voltage dependency of the Q(V) control (compare Section III.D).

V. Sensitivity Analysis

The scope of the sensitivity analysis is the cloudy sky day scenario with the PV RPC strategies PF(P) and Q(V) control. Table I gives an overview of the simulation assumptions for the sensitivity scenarios (S1 to S10). The results of the sensitivity analysis are given in Fig. 12. In Fig. 12 the black lines show the result of the reference scenario and the grey bars describe the change for the respective sensitivity. Here, only the mean value of the result population is considered. The results for the scenario without PV RPC (PF=1) are also shown in the Fig. 12 (plus sign). The focus is set especially on the relevant impact factors on the number of OLTC switching operations.

A. *Increase of OLTC Switching Operations*

The increase of solar variability in the MV grid area (S1) leads only to a slight increase of the number of OLTC switching operations (PF(P) control). Here, the delay function of the OLTC controller avoids additional OLTC switching operations in case of short term voltage fluctuations at T1.

The number of OLTC switching operation is especially sensitive to the applied PV penetration scenario (S3, S4). An increase of the PV nominal power leads to a relevant increase of OLTC switching operations, especially for the PF(P) control. For sensitivity scenario S3 and S4, the PV systems provide an even higher reactive energy for the Q(V) control than for the PF(P) control, due to the high grid voltages. Nevertheless, the Q(V) control just lead to a slight increase of

This article has been accepted for publication in a future issue of this journal, but has not been fully edited. Content may change prior to final publication. Citation information: DOI 10.1109/TSG.2017.2712633, IEEE Transactions on Smart Grid

OLTC switching operations in this high PV penetration scenarios (S4).

The position of the PV systems in the grid affects especially the Q(V) control. In case the PV systems are situated especially at weak grid nodes (end of feeders, S6) the PV systems will provide more reactive power due to the high grid voltages. This can increase the impact of Q(V) control on the OLTC operation. However, even for the applied extreme scenario with two large PV systems (2 x 4.4 MW) at the end of the two feeders (node T11, T6), the Q(V) control just leads to a slight increase of OLTC switching operations.

A comparable result is achieved for an adjusted Q(V) control (S7), whereby the reactive power provision of the PV systems starts at lower grid voltages and the PV reactive power provision increases. Nevertheless, the Q(V) control just cause a minor increase of OLTC switching operations.

Furthermore, a relevant increase of the number of OLTC switching operations is determined for a weak external grid interconnection (S10, with low short circuit power of external grid element). However, here also the scenario without PV RPC (PF=1) is affected.

B. Decrease of OLTC Switching Operations

A relevant decrease of the number of OLTC switching operations (PF(P) control) is achieved with a adjusted OLTC transformer setting (especially S8). In the reference scenario the OLTC deadband (dV_{OLTC_BAND} = 2 %) is not much larger than the voltage change per OLTC tap (dV_{OLTC_tap} = 1.51 %). The voltage reserve at T1 after an OLTC switching operation is rather small in the reference scenario ($V_{T1\_reserve}$ = dV_{OLTC_BAND} - dV_{OLTC_tap} = 0.5 %). Therefore, induced voltage variations by PV systems larger than 0.5 % at T1 can already cause repeated OLTC switching operations. This effect is explained more in detail in the Appendix in Fig. A3 and in [18]. In order to increase the voltage reserve at T1 after an OLTC switching operation, the OLTC deadband can be increased or the voltage change per OLTC tap can be decreased. An increase of the OLTC deadband might conflict with the voltage regulation scheme in the distribution grid and the adoption of the voltage change per OLTC tap might require a new OLTC transformer. In the sensitivity scenario S8 the voltage reserve at T1 ($V_{T1\_reserve}$ = dV_{OLTC_BAND} - dV_{OLTC_tap} = 0.8 %) was increased by a reduced voltage change per OLTC tap (dV_{OLTC_tap} = 1.2 %), which lead to a relevant reduction of OLTC switching operations for the PF(P) control (S8).

The adjustments of the delay function of the OLTC transformer (S9, delay_V2) with an extended delay time just lead to a slight decrease of OLTC switching operations.

A relevant decrease of OLTC switching operations is also determined for an adjusted PF(P) control (S7, PFP_V2). With the characteristic PFP_V2 the reactive power gradients of the PV systems (dQ/dP) are reduced compared to the scenario with PF(P)_V1 (compare Fig. 7, left). Nevertheless, the adjustment also leads to an increased reactive energy provision of the PV systems and to a reduced effectiveness ratio Eff_Q.

Furthermore, a reduced solar variability (S2) in the MV grid area leads to a small decrease of OLTC switching operations.

TABLE I
OVERVIEW SIMULATION ASSUMPTIONS SENSITIVITY ANALYSIS

Scenario	Category	Setting
Ref.	Reference	According to Table II
S1	Increased solar variability	Time constant T = 150 s
S2	Reduced solar variability	Time constant T = 500 s
S3	Increased PV penetration 1	$P_{PV\_STC} = S_N$ = 1.0 MVA
S4	Increased PV penetration 2	$P_{PV\_STC} = S_N$ = 1.2 MVA
S5	PV location at beginning of feeders	2 PV systems (2 x S_N = 4.4 MVA) at T1 and T2
S6	PV location at end of feeders	2 PV systems (2 x S_N = 4.4 MVA) at T6 and T11
S7	RPC control (Fig. 4)	PF(P): PFP_V2 Q(V): QV_V2
S8	OLTC control	Voltage per tap = 1.2%
S9	OLTC control	Delay function V2 applied (Fig. 5, left)
S10	External Grid (weak HV connection)	Internal impedance: R= 3.6 Ω, X=11.5 Ω (Sk" at T_0= 1 GVA)

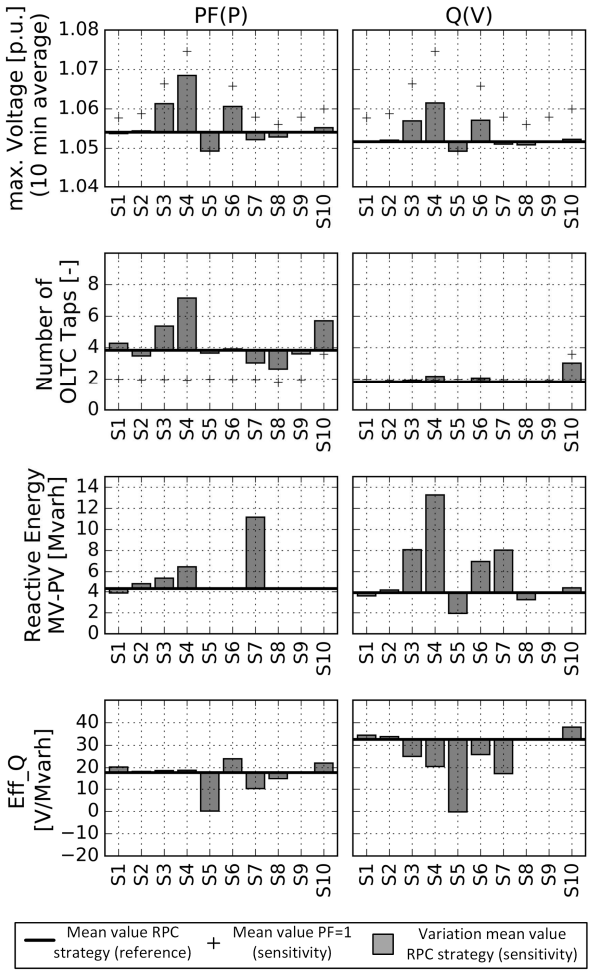

Fig. 12: Result of the sensitivity analysis for the PF(P) control (left) and Q(V) control (right).

C. Conclusion Sensitivity Analysis

The different sensitivity scenarios affect the maximum grid voltage, the PV reactive power provision, the number of

OLTC switching operations and the effectiveness ratio Eff_Q. A suitable configuration of the local control characteristics is always a compromise between these impact factors and their priorities. Nevertheless, it should be pointed out, that the Q(V) control shows in all investigated scenarios a rawer low impact on the number of OLTC switching operations and achieves in most investigated scenarios a rather high effectiveness ratio compared with a PF(P) control.

VI. Discussion of Results

In this section, the simulation assumptions and the relevance of the presented findings are discussed and general conclusions are derived.

In Section III.E a first assessment was proposed to analyze the impact of PV RPC on the VR control. In the present investigation, the VR (OLTC transformer) controls the voltage at a grid node, which is especially sensitive to the reactive power flow. Therefore, the reactive power fluctuations by PV RPC lead to an increase of voltage variations at the controlled grid node and cause an increase of OLTC switching operations. The presented findings are relevant for similar VR and grid configurations.

An increase of OLTC switching operations can accelerate the abrasion of the OLTC and can shorten the OLTC maintenance intervals. However, traditional tap changers for oil immersed transformers usually have a mechanical lifetime of 800,000 operations and maintenance intervals of 50,000 to 100,000 operations or 7 years [27], [28]. Hence, the determined number of OLTC switching operations (maximum 12 taps/day with PF(P) control) seems to remain in an acceptable range for the applied simulation model. However, a high sensitivity of the simulation results is determined for the PV penetration scenario and additional PV installations with RPC will further increase the number of OLTC switching operations. It should be highlighted that the applied simulation model corresponds to a medium PV penetration scenario (PV capacity over peak load: 36 %). Therefore, the analysis is especially relevant for distribution grids with a medium or high PV penetration and a system wide rollout of PV RPC.

A similar methodology was applied in a preliminary study [18] for a real German MV grid and the results show similar trends with a relevant increase of OLTC switching operations for fixed PF control (PF=0.95) and PF(P) control and a low increase for the Q(V) control. So the applied methodology is also applicable for real distribution grids. In [18] also high time resolution solar irradiation data at different grid nodes were available and the active and reactive power flow at the OLTC transformer was validated with grid measurements. For the applied generic grid model, the aim was not a detailed replication of a real MV grid. In the paper at hand, the distributed PV fleet was modelled with an adjustable low pass filter (Section II.C.), which represents the smoothing effect of solar variability in the MV grid area. With this simplified approach, the impact of solar variability on the parallel operation of OLTC control and PV RPC can be analyzed and the approach can be used in case no comprehensive measurement data is available. It should be highlighted that an accurate modelling of a distributed PV fleet requires comprehensive measurement data (e.g. solar irradiation data at different grid locations with high temporal resolution, e.g. [22], [18]), which is usually not available.

The simulation results are case sensitive to the applied simulation model. Nevertheless, a number of general conclusions can be derived from the study.

- The additional OLTC switching operations by PV RPC have usually a contrary effect on the grid voltage then the PV reactive power provision (see Section IV.C) → unintended OLTC switching operations.
- The unintended OLTC switching operations by PV RPC therefore reduce the effectiveness in parallel operation of OLTC control and PV RPC (see Section IV.C).
- The voltage dependency of the Q(V) characteristic also tends to smooth voltage variations at grid nodes, which are directly coupled with the PV network connection point (see Section III.D). This effect can avoid or reduce the risk of unintended OLTC switching operations.
- The PF(P) control shows within the highest reactive power gradients (dQ/dP) of the PV systems (see Section III.C). This effect can increase the risk of additional OLTC switching operations.

In a smart grid environment coordinated control approaches of PV systems and voltage regulators can generally improve the effectiveness in the parallel operation of different control entities and can avoid or reduce unintended interactions. Nevertheless, even in a highly integrated grid, autonomous control approaches will further play an important role, due to fast response time, no necessary communication links and a simple parameterization and application. Therefore, the applied assessment methodology can support the identification of suitable autonomous control configurations.

VII. Conclusion

In this paper we presented a technical assessment of the parallel operation of an autonomous voltage regulator control (OLTC control) and autonomous PV reactive power control (RPC). The investigated control strategies encompass a voltage mode of the OLTC transformer and different PV RPC strategies (fixed PF, PF(P) and Q(V) control).

The technical assessment is performed by a Monte Carlo simulation of the external grid voltage and according to the criteria of maximum grid voltage, PV reactive power provision, and number of OLTC switching operations. Furthermore, an effectiveness ratio for the parallel operation of OLTC control and PV RPC was introduced.

We showed that PV RPC can cause unintended OLTC switching operations, which reduce the effectiveness ratio and overall increase the number of OLTC switching operations. Furthermore, we pointed out that the impact of PV RPC on the number of OLTC switching operations is highly sensitive to the applied PV RPC strategy. In the applied case study the Q(V) control showed a rather low impact on the number of OLTC switching operations and achieved a rather high effectiveness ratio compared with a PF(P) control. This outcome was approved by a sensitivity analysis of grid configurations and controller settings. Finally, we discussed the simulation assumptions and the relevance of the presented findings for grid operation.

This article has been accepted for publication in a future issue of this journal, but has not been fully edited. Content may change prior to final publication. Citation information: DOI 10.1109/TSG.2017.2712633, IEEE Transactions on Smart Grid

APPENDIX

ANNEX

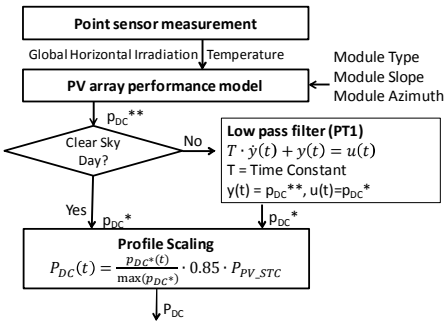

Fig. A1: Flow chart for the preparation of the PV generator profiles (P_{DC}). The reduction of solar variability by a low pass filter is only required for the cloudy day. Finally, the PV generator profiles are scaled to a maximum peak power of 85 % of the nominal generator power under standard test conditions (P_{PV_STC}). In the study [22] it is determined, that the maximum aggregated power of a PV fleet in the MV and LV level do not exceed 85 % of the aggregated nominal generator power ($P_{PV\ STC}$) in the majority of cases.

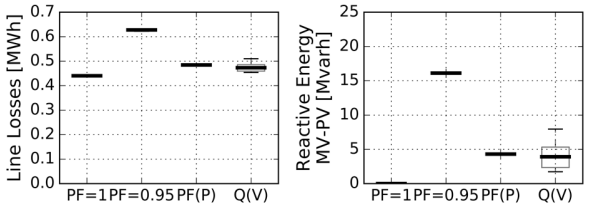

Fig. A2: Box plot of grid losses (left, only line losses considered) and reactive energy provision of PV systems (right) for the cloudy sky day

TABLE AI
GENERAL SIMULATION ASSUMPTIONS (REFERENCE CASE)

	Category	Setting
OLTC Transformer	Rated power	40 MVA
	Rated voltage	110 kV / 20 kV
	Impedance	r=0.00491 p.u., x=0.1651p.u.
	Vector group	Ynd5
	Add. voltage per tap	dV_{OLTC_tap} = 1.51 %
	Max./min. tap position	± 15
PV Profile	Measurement Values	Global horizontal irradiation, temperature
	Measurement resolution	3 s [1]
	Measurement location	Southern Bavaria (D)
	PV array performance model	According [26]
	Module type	Shell Solar SM100 12
	Module slope, azimuth	28°, 0° South
	Time constant	300 s
PV Inverter	Nominal power S_N	800 kVA
	Max. reactive power	0.312 S_N
	Min. capable power factor	0.2
	Time constant PT1 P	1 s
	Time constant PT1 Q	5 s
	Effectivity according [2]	For SMA mini central
Ext. grid	Bus type	Slack
	Internal impedance	R=0 Ω, X= 0Ω (ideal)
	Set voltage	Normal distribution, μ=1.0 p.u., σ=0.05 p.u. (values are limited afterwards, between 0.85 p.u. and 1.15 p.u.)

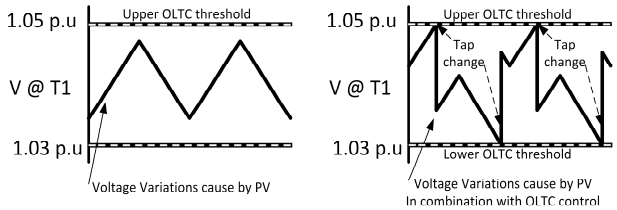

Fig. A3: The figure shows exemplary the impact of voltage variations at T1 for two different external grid voltages. The voltage variations at T1 solely caused by PV are in both cases equal. However in the left example no OLTC tap change is triggered, because the voltage variations at T1 are around the OLTC set value of 1.04 p.u.. In a best case example voltage variations at T1 of up to 2% of V_N (dV_{OLTC_BAND}) would cause no additional OLTC switching operation. Otherwise, in the right example four OLTC tap changes are triggered; because the voltage variations at T1 are around the OLTC thresholds. In a worst case example voltage variations at T1 above 0.49% V_N (dV_{OLTC_BAND} of 2% V_N minus dV_{OLTC_tap} of 1.51% V_N) can already cause a repeated tripping of the OLTC transformer.

REFERENCES

[1] IRENA (2015, December). *Data and Statistics* [Online]. Available: http://resourceirena.irena.org/gateway/dashboard/

[2] M. Braun, "Provision of Ancillary Services by Distributed Generators," Ph.D. dissertation, Dept. of Elect. Eng. and Comput. Sci., Univ. of Kassel, 2008.

[3] C. Schauder (2014, March). *Advanced Inverter Technology for High Penetration Levels of PV Generation in Distribution Systems.* [Online]. Available: http://www.nrel.gov/docs/fy14osti/60737.pdf

[4] German Energy Agency (2012, December). *dena – Verteilnetzstudie: Ausbau und Innovationsbedarf der Stromverteilnetze in Deutschland bis 2030.* [Online]. Available: http://www.dena.de/projekte/energiesysteme/verteilnetzstudie.html.

[5] T. Stetz, K. Diwold, M. Kraiczy, D. Geibel, S. Schmidt, M. Braun, "Techno Economic Assessment Approach for Autonomous Voltage Control Strategies in Low Voltage Grids," *IEEE Trans. on Smart Grid*, Vol. 5, No.4, July 2014.

[6] T. Stetz, *"Autonomous Voltage Control Strategies in Distribution Grids with Photovoltaic Systems – Technical and Economical Assessment,"* Ph.D. dissertation, Energy Manage. and Power Syst. Operation, Univ. of Kassel, 2013.

[7] H. Brunner, A. Lugmaier, B. Bletterie, H. Fechner, R. Bründlinger (2010, December). *DG DemoNetz – Konzept*. [Online]. Available: http://download.nachhaltigwirtschaften.at/edz_pdf/1012_dg_demonetz_konzept.pd

[8] *Power generation systems connected to the low voltage distribution network*, VDE AR N 4105, 2011.

[9] *Technical Guideline for the Connection and Parallel Operation of Generator Connected to the Medium Voltage Network*, German association of energy and water industries (BDEW), 2008.

[10] *Technische und organisatorische Regeln für Betreiber und Benutzer von Netzen – Hauptabschnitt D4*, TOR D4, 2013.

[11] *Requirements for micro generating plants to be connected in parallel with public low voltage distribution networks*, EN 50438, 2014.

[12] E. Wieben et al., "Weiterentwicklung der Anforderungen an Erzeugungsanlagen im Niederspannungsnetz," (in German) Netzpraxis No. 6, 2012.

[13] R. A. Walling, R. Saint, C. R. Dugan, J. Burke, L. A. Kojovic, "Summary of Distributed Resources Impact on Power Delivery Systems," *IEEE Trans. on Power Delivery*, Vol. 23, No. 3, July 2008.

[14] F. Andren, B. Bletterie, S. Kadam, P. Kotsampopoulos, and C. Bucher, "On the Stability of Local Voltage Control in Distribution Networks With a High Penetration of Inverter Based Generation," IEEE Trans. Ind. Electron., vol. 62, no. 4, pp. 2519–2529, Apr. 2015.

[15] L. Kojovic, "Modern Techniques to Study Voltage Regulator – DG Interactions in Distribution Systems," *Transmission and Distribution Conf. and Exposition IEEE/PES*, 2008.

[16] Y. P. Agalgaonkar, B. C. Pal, R. A. Jabr, "Distribution Voltage Control Considering the Impact of PV Generation on Tap Changers and Autonomous Regulators," *Trans. on Power Systems*, Vol.29, No.1, January 2014.

[17] B. Mather, "Quasi static time series test feeder for PV integration analysis on distribution systems," *IEEE Power and Energy. Society*

General Meeting, San Diego, CA, 2012, DOI: 10.1109/PESGM.2012.6345414
[18] M. Kraiczy, M. Braun, G. Wirth, T. Stetz, J. Brantl, S. Schmidt, "Unintended Interferences of Local Voltage Control Strategies of HV/MV Transformer and Distributed Generators," *28th European PV Solar Energy Conf. and Exhibition*, Paris, 2013.
[19] M. Hartung, E. M. Baerthlein, A. Panosyan, "Comparative Study of Tap Changer Control Algorithms for Distribution Networks with high Penetration of Renewables", *CIRED Workshop*, Rome, 2014.
[20] K. Rudion, A. Orths, A. Styczynski, K. Strunz, "Design Benchmark of Medium Voltage Distribution Network for Investigation of DG Integration," *Power Eng. Society General Meeting*, Montreal, 2006.
[21] J. V. Milanović, K. Yamashita, S. M. Villanueva, S. Ž. Djokić, Lidija M. Korunović, "International Industry Practice on Power System Load Modeling," *IEEE Trans. on Power Systems*, Vol. 28, No. 3, August 2013.
[22] G. Wirth, "Modellierung der Netzeinflüsse von Photovoltaikanlagen unter Verwendung meteorologischer Parameter," Ph.D. dissertation, Faculty of Math. and Natural Sci., Univ. of Oldenburg, 2014.
[23] M. Lave, J. Kleissl, S. J. Stein, "A Wavelet based Variability Model (WVM) for Solar PV Power Plants," *IEEE Trans. on Sustainable Energy*, Vol. 4, No. 2, April 2013.
[24] J. Marcos, L. Marroyo, E. Lorenzo, M. Garcia, "Smoothing of PV power fluctuations by geographical dispersion," in *Progress in Photovoltaics: Research and Applications*, DOI: 10.1002/pip.1016.
[25] T. Stetz, M. Braun, H. J. Nehrkorn, M. Schneider, "Methods for maintaining voltage limitations in medium voltage systems," *ETG Conference*, Würzburg, 2011.
[26] D. L. King, W. E. Boysen, J.A. Kratochvill (2004, December). *Photovoltaic Array Performance Model* [Online]. Available: http://prod.sandia.gov/techlib/access control.cgi/2004/043535.pdf
[27] *On Load Tap Changers for Power Transformers*, Maschinenfabrik Reinhausen, Regensburg, 2013.
[28] *Type CM2 Vaccum On Load Tap Changers for oil immersed transformer*, Shanghai Huaming Power Equipment Co., Ltd., Shanghai, 2010.
[29] *Technical requirements for the connection and operation of customer installations to the high voltage network*, VDE AR N 4120, 2015.
[30] M. Kraiczy, T. Stetz, H. Wang, S. Schmidt, and M. Braun, "Entwicklung des Blindleistungsbedarfs eines Verteilnetzes bei lokaler Blindleistungsregelung der Photovoltaikanlagen im Niederspannungsnetz," ETG Congress, Kassel, Germany, March 2015.

AUTHOR INFORMATION

Markus Kraiczy was born in Germany in 1983. He received his B.Eng. in Electrical Engineering from the University of Applied Sciences Anhalt and his M.Sc. in Renewable Energies and Energy Efficiency from the University of Kassel in 2012. He is now a research associate with the Fraunhofer Institute for Wind Energy and Energy System Technology (IWES) in Kassel, Germany.

Thomas Stetz was born in Germany in 1983. He received a Diploma in Industrial Engineering (Dipl.-Wi.-Ing (FH)) from the University of Applied Sciences in Darmstadt in 2008 and a M.Sc. in Renewable Energies and Energy Efficiency from the University of Kassel in 2009. He worked with Fraunhofer IWES from 2009 to 2015 and received a PhD in Electrical Engineering from the University of Kassel in 2014. At present, Thomas Stetz is Professor for Smart Grids and Energy Storage at the University of Applied Sciences Mittelhessen in Gießen, Germany.

Martin Braun (senior member IEEE) was born in Germany in 1978. He received a Diploma in Electrical Engineering and a Diploma in technically oriented Business Administration from the University of Stuttgart. In 2008, he received his Ph.D. from the University of Kassel. Martin Braun is now Professor for Energy Management and Power System Operation at the University of Kassel and head of the department "Distribution System Operation" at the Fraunhofer IWES in Kassel, Germany.